Available online at www.sciencedirect.com
ScienceDirect
Carbohydrate Research 342 (2007) 1726–1740
Carbohydrate RESEARCH

DFT studies of the ionization of alpha and beta glycopyranosyl donors

Dennis M. Whitfield*

Institute for Biological Sciences, NRC Canada, 100 Sussex Drive, Ottawa, ON, Canada K1A 0R6

Received 19 February 2007; received in revised form 26 April 2007; accepted 6 May 2007
Available online 18 May 2007

Abstract—Current attempts at mimicking the transition states (TSs) of glycosyl processing enzymes (GPEs) that proceed through TSs with a high degree of oxacarbenium ion formation suffer from a paucity of data about the conformations of such oxacarbenium ions. Because TSs are maxima, the current models based on minimized structures may need some refinement. As part of studies directed at optimizing chemical glycosylation the ionization of 3,4,6-tri-*O*-acetyl-α/β-D-glucopyranosyl chlorides and triflates, 2,3,4,6-tetra-*O*-methyl-α/β-D-glucopyranosyl fluorides, chlorides and triflates, 2,3,4,6-tetra-*O*-methyl-α/β-D-mannopyranosyl fluorides, 2,3-di-*O*-methyl 4,6-*O*-benzylidene α/β-D-mannopyranosyl triflates and 2,3-di-*O*-methyl 4,6-*O*-benzylidene α/β-D-glucopyranosyl triflates was studied by a prototypic density functional theory (DFT) procedure. In all cases, the α-anomers ionized smoothly to $^4H_3$ half chair conformations or adjacent envelopes. By contrast, all β-anomers exhibited an abrupt conformational change before ionization was complete. The nature of the conformations sampled depends on both the leaving group and the protecting group. The methods presented can be readily adapted to the study of any GPE or chemical glycosylation and provide a method for initial evaluation of plausible TSs, which in turn can be used in mimetic design.

Keywords: Glycosylation; Oxacarbenium ions; Transition states; Glycosyl processing enzymes; Density functional theory

1. Introduction

It is generally assumed that if one can mimic the TS of an enzyme-catalyzed reaction with suitable substrate like molecules, then such molecules should be good TS inhibitors of this enzyme.[1] Such inhibitors can take advantage of both enthalpic and entropic factors because the $\Delta G^{\ddagger}$ associated with the rate limiting step of the enzyme-catalyzed reaction contains both terms. The enthalpic portion of this energy is usually associated with the binding energy of the substrates or inhibitors at the TS, whereas the entropy is frequently associated with binding site preorganization and solvation terms. For glycosyl processing enzymes (GPEs) that go through glycopyranosyl oxacarbenium ion intermediates, discussions about TS mimics have centred around mimicking 'flat' glycopyranosyl ions, such as the $^4H_3$ half chairs shown for the D-*gluco* (**1**) and D-*manno* (**2**) configured species in Scheme 1 and mimicking the positive charge.[2] However, as more and more GPEs have been studied in detail, it has become apparent that many enzymes likely have ring conformations at their TSs other than D-$^4H_3$ and L-$^3H_4$.[3] This has led to a refinement of the strategy for modeling glycopyranosyl oxacarbenium ion TSs to include ring conformations that maintain the C-5–O-5–C-1–C-2, τ_5, ring torsion angle to near 0°. In addition to $^4H_3$ and $^3H_4$ half chairs and their adjacent in conformational space ^4E and E_3 or ^3E and E_4 envelopes, this includes the $^{2,5}B$ and $B_{2,5}$ boat conformations.[4] Among skew conformations the pairs $^2S_0$ and $^5S_1$, and $^0S_2$ and $^1S_5$ have optimum values[5] of τ_5 of ±30° and are close in conformational space to $^{2,5}B$ and $B_{2,5}$ respectively, and so are also sometimes considered.[6] A visualization of this conformational space can be seen in the three-dimensional representations of the trajectories presented below.

* Tel.: +1 613 993 5265; fax: +1 613 952 9092; e-mail: dennis.whitfield@nrc.ca

0008-6215/$ - see front matter
doi:10.1016/j.carres.2007.05.012

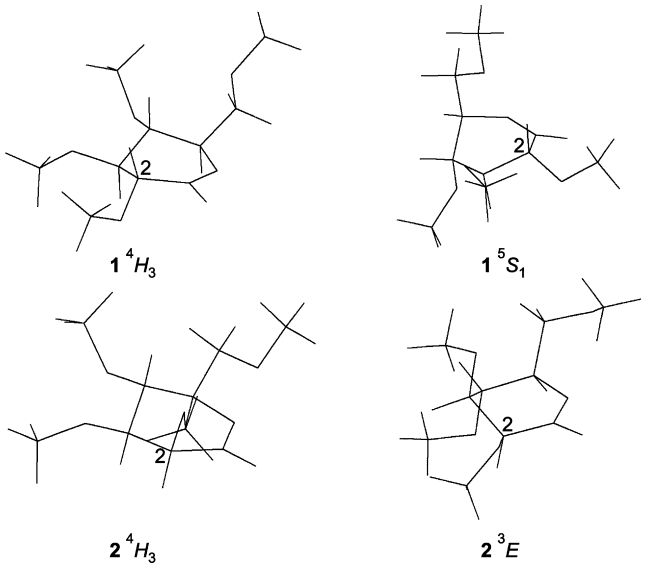

Scheme 1. Stick representations of two conformers of the glycopyranosyl oxacarbenium ions of D-*gluco* (**1**) and D-*manno* (**2**). Note the equatorial position of the C-2–O-2 bond in all but **2** $^4H_3$ and the *syn* orientation of CH-2–C-2–O-2–CH-3 in all cases. C-2 is labeled in all structures for clarity.

Our interest in glycopyranosyl oxacarbenium ions arose from studies directed at identifying factors that synthetic chemists could control with the aim of both minimizing side reactions and maximizing stereoselectivity in glycosylation reactions.[7] To date, the factors identified have revolved around the position and nature of the protecting groups on glycosyl donors. As well, two additional stabilizing conformational preferences have been identified namely, that O-2 of glycopyranosyl oxacarbenium ions has a preference for being equatorial and hence in the plane defined by the O-5–C-1 double bond, and that the exocyclic torsion angle CH-2–C-2–O-2–H or C has a strong preference for *syn* conformations.[8] The first preference has led to the identification of the importance of the $^5S_1$ conformations of D-*gluco* (**1**) configured ions. For D-*manno* (**2**) the different configuration at C-2 allows the ^3E conformation to maximize this preference, Scheme 1.[7b] The possible importance of the conformational preferences about C-2–O-2 has not led to any identifiable strategies, but it does suggest a subtle conformational biasing mechanism for affecting the reactivity of glycosyl donors in glycosylation reactions. It is also plausible that GPEs could use this stabilization in some cases. One probable example has been identified.[9]

All of the above discussion revolves around static structures. In fact, even the glycopyranosyl oxacarbenium ion structures shown in Scheme 1 are minima on their respective potential energy surfaces, PES. This is in contrast to the fact that TSs are characterized by one imaginary frequency where the components of this unique frequency correspond to specific atoms of the molecules and their motions at the TS. Although there are numerous ad hoc discussions in the literature about the motions associated with arriving at the TS, there is little experimental or computational data known.[10] This communication presents our first attempts at mimicking the approach to ions like **1** and **2**. By necessity this approach is limited by the computational resources available and the algorithms available to model the current hypotheses.

Because our primary interest is the synthetic chemical glycosylation reaction, the cases to be studied are protected glycosyl donors with leaving groups (X) at C-1 that have been used in glycosylation reactions. Most previous computational attempts at studying glycopyranosyl ionization have studied acid-catalyzed processes where the exocyclic oxygen is first protonated.[11] One such study showed that C-1–O-1 bond breaking was synchronous to O-5–C-1 double bond formation[12] and a different behaviour for each anomer was found.[13] In our case, ionization is achieved by stepwise elongation of the C-1–X bond with full geometry optimization at each point. Solvent is considered by a continuum dielectric approximation. Initial attempts to do such seemingly trivial C-1–X bond elongation calculations universally failed because as the leaving group acquired more and more negative charge it would move during the stepwise optimization process to approach positive dipoles, such as the various C–H groups in the glycosyl donors. In extreme cases, base-catalyzed elimination reactions would occur. To overcome this problem a positively charged Li^+ ion was added as a 'promoter' to partially neutralize the developing negative charge. Further geometric constraints on the position of the Li^+ ion had to be made to avoid unwanted movements of the Li^+ ion towards electronegative atoms of the glycosyl donor during the stepwise optimization process, which sometimes also led to unrealistic species. With this prototypic system several glycopyranosyl molecules were stepwise ionized. In this way, a first attempt to assess the validity of some of the existing ad hoc descriptions of glycopyranosyl ionization could be made.

2. Methods

The DFT calculations were carried out with the Amsterdam density functional (ADF) program system, ADF2005.[14] The atomic orbitals were described as an uncontracted triple-ζ Slater function basis set with a single-ζ polarization function on all atoms, which were taken from the ADF library (TPZ). The basis set dependence of the results was tested with glycopyranosyl triflates using the C-1–O(S) and (C-1)O–S bond lengths as criteria. The TPZ basis set, which is the largest available in ADF, gave the most realistic values of these parameters (not shown).[15] A set of s, p, d, f and g Slater functions centred on all nuclei were used to fit the electron

density, and to evaluate the Coulomb and exchange potentials accurately in each SCF cycle. The local part of the V_{xc} potential (LDA) was described using the VWN parametrization,[16] in combination with the gradient corrected (CGA) Becke's functional[17] for the exchange and Perdew's function for correlation (BP86).[18] The CGA approach was applied self-consistently in geometry optimizations. Second derivatives were evaluated numerically by a two-point formula. The solvation parameters (CH_2Cl_2) within the COSMO procedure were dielectric constant $\varepsilon = 9.03$, ball radius = 2.4 Å, or H_2O $\varepsilon = 78.4$, ball radius = 1.3 Å; with atomic radii of C = 1.989, O = 1.7784, H = 1.3 Å, Li = 2.1294 Å, F = 1.7199 Å, S = 2.106 Å, Cl = 2.0475 Å.

Initial geometries all started with protected D-glycopyranosyl donors in $^4C_1$ conformations with all side chains (protecting groups) in minimum energy conformations. All calculations used internal coordinates. The Li^+ ion was positioned at a fixed distance from the leaving groups: 1.8 Å (OTf), 1.8 Å (F) and 1.9 Å (Cl). The Li^+ leaving group distances were chosen by trial and error preliminary calculations (not shown). A fixed bond angle extending out from the leaving group with values at or near the approximate tetrahedral value of 109° was also used. Finally a fixed torsion angle of 179.9° was used to keep the Li^+ ion as far as possible from the glycosyl donor while maintaining adequate overlap to neutralize the developing negative charge of the leaving group. The initial structures were fully optimized with these constraints. However, these non-physical constraints mean that these are not minima on their respective PES. The step size was chosen to be as small as possible to allow for ionization without abrupt discontinuities but large enough to keep the computation resources manageable, typically about 0.03 Å. All ionizations were also run in reverse to test for reversibility.

3. Results

3.1. Ring conformations

Lemieux hypothesized that 3,4,6-tri-*O*-acetyl-α-D-glucopyranosyl chloride (**3a**) ionized under solvolysis conditions to a $^4H_3$ oxacarbenium ion analogous to **1** above.[19] Similarly, he hypothesized that the β-chloride (**3b**) ionized to the $^3H_4$ oxacarbenium ion. This analysis was based on the observation of first-order kinetics consistent with a S_N1-like mechanism for both chlorides. However, the α-chloride gave the β-acetate as product and the β-chloride the α-acetate. The observed stereochemical outcome was hypothesized to arise from facially selective nucleophilic attack on the two conformers of the oxacarbenium ions. Other authors have also presented evidence for facial selectivity of nucleophilic attack on pyranosyl oxacarbenium ions including experimental data that suggests that at the limit of diffusion control such stereoselectivity is lost.[20] Our static computational studies of glycopyranosyl oxacarbenium ions have consistently found at least two minimum energy conformations of such species, the 'two conformer hypothesis'.[7b] In a previous report using ab initio molecular dynamics (AIMD) it was found for *gluco* and *manno* configured ions **1** and **2** that low energy pathways connect these two conformers, $^4H_3$–$^5S_1$ and $^4H_3$–^3E, respectively.[7a] Thus, once ionized, and if lifetimes are long enough, such ions can conformationally interconvert. However, the Lemieux hypothesis outlined above suggests that the two conformers could also arise from direct ionization. Thus, the **3ab** system seemed like an ideal test to see if the two conformers could form by ionization of different anomers as well as by interconversion.

Figure 1a and b shows a superimposition of the frames for the forward and reverse **3a** C-1–Cl bond elongation (contraction); both series are essentially superimposable. Closer examination of this figure demonstrates that the majority of the motion involves C-5, O-5, C-1 and C-2, as well as rotation about C-2–O-2. Figure 2a–u and Table 1, Supplementary data show selected geometric parameters from frames from these stepwise calculations. The numbers (-#) after the hyphens refer to the frame number where b# refers to contraction calculations and are included to allow cross reference between Tables 1 and 3. Table 2, Supplementary data has the six ring dihedral angles that were used to calculate the ring descriptors tabulated in Table 3, Supplementary data. For **3a** τ_5 changes from −44° to −5.1° as it approaches planarity, leading to a ^4E envelope conformation at maximum C-1–Cl bond elongation. This trajectory is shown in a three-dimensional spherical representation in Figure 3a. It is also apparent from Figure 1a that the Cl^- ion moves under the ring presumably to maximize C–H dipolar interactions with CH-3 and CH-5, in spite of the Li^+ promoter. Without the Li^+ ion or the geometric constraints described in the experimental section, this type of dipole–ion interaction led to ring conformation distortions and in extreme cases to elimination reactions. However, an examination of the relative energies versus bond length for the C-1–Cl shows no minima associated with these ion–dipole effects, Figure 4a. The relevance of such weak interactions to real chemical reactions where competing interactions of the leaving group with typical reaction components such as solvent, hindered bases, molecular sieves and promoters take place, is difficult to predict with certainty.

For this reason, similar bond elongation computations were performed with a different leaving group namely trifluoromethanesulfonate (triflate, Tf), that is, 3,4,6-tri-*O*-acetyl-α/β-D-glucopyranosyl triflates (**4ab**), see Figure 2b, d and f. Glycosyl triflates have been suggested to be the true glycosyl donors under a variety of

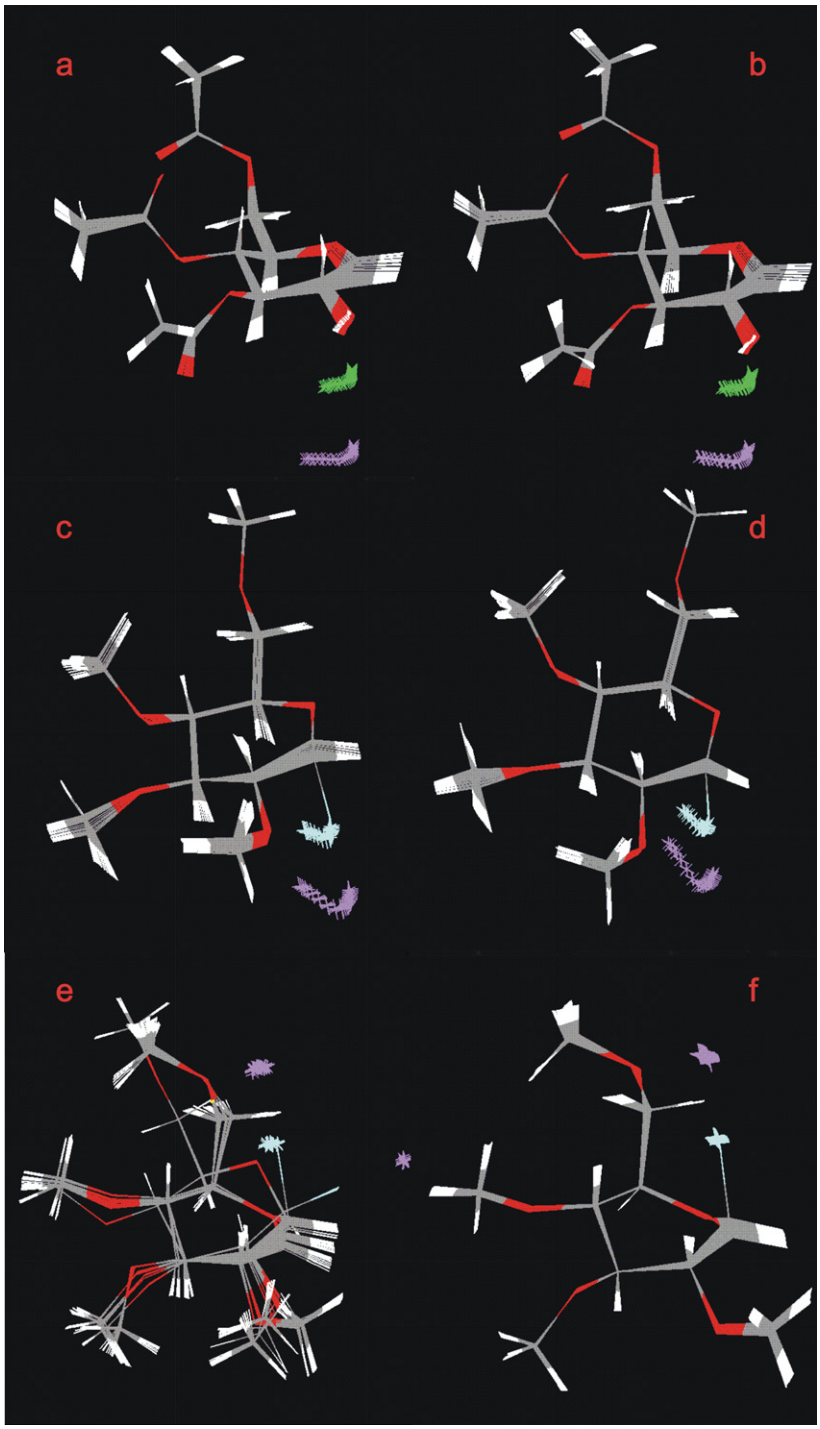

Figure 1. Superimpositions of C-1–X bond elongations (contractions) for (a) **3a** elongation; (b) **3a** contraction; (c) **5a** elongation; (d) **5a** contraction; (e) **5b** elongation; (f) **5b** contraction. Element colours: C, grey; H, white; O, red; Cl, green; Li, purple; F, pale blue.

glycosylation conditions and so they are of considerable interest to study.[21] One QM study supported the possibility that anomeric triflates are displaced in a S_N2 manner by nucleophilic alcohols without going through discrete oxacarbenium ion intermediates.[22] The possibility that triflate oxacarbenium ion pairs are the reactive species has also been suggested. Triflate **4a** smoothly and reversibly ionizes to an ion with the $^4H_3$ half chair conformation, see Figure 2b. These combined results for **3a** and **4a** fit Lemieux's hypothesis for the α-chloride.

Figure 5a–f shows selected frames from the same elongation process for the β-chloride **3b**. For the first few frames (Fig. 5a and b) the $^4C_1$ conformation of the neutral donor is maintained. At a C-1–Cl bond length of

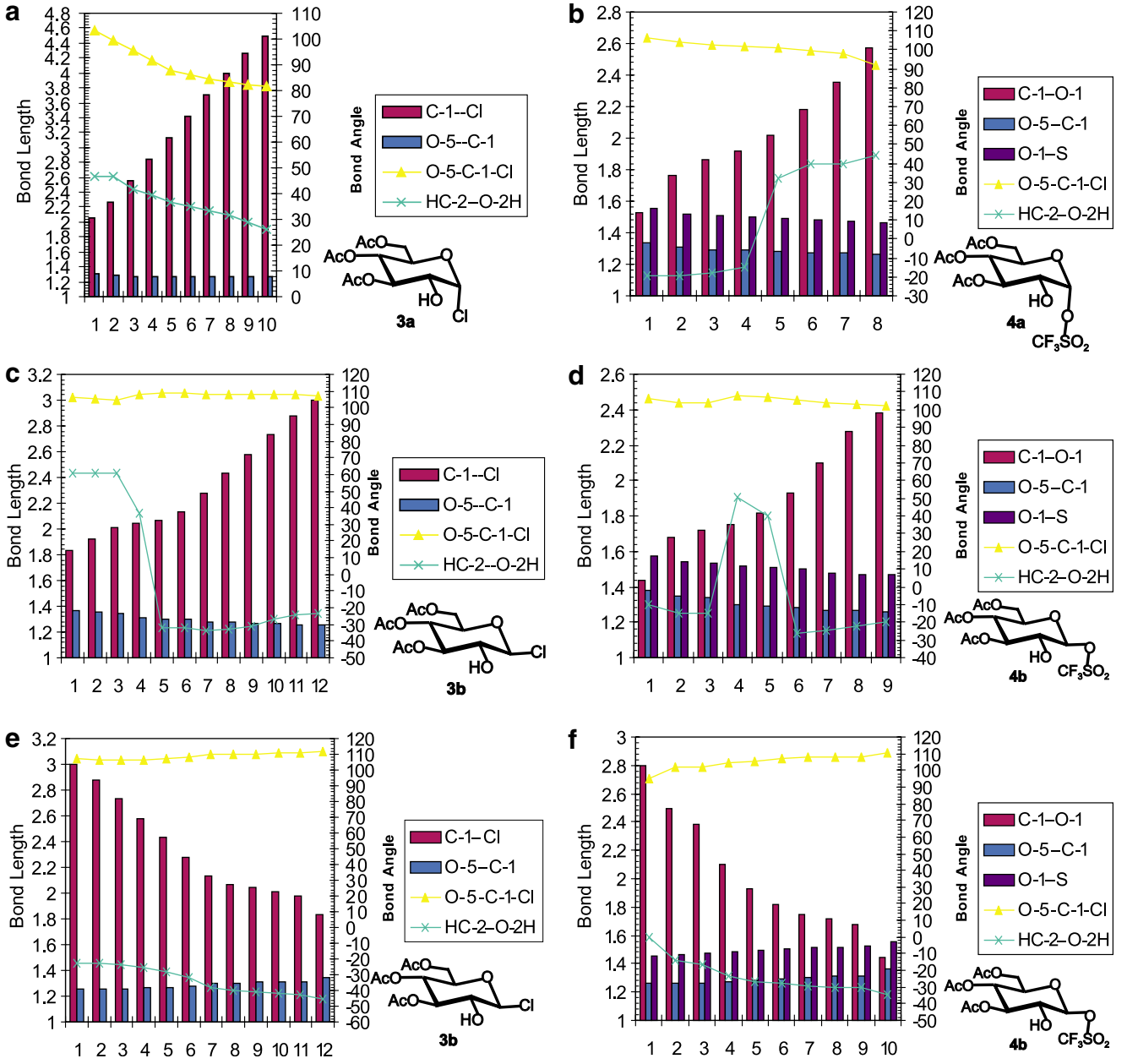

Figure 2. Selected geometric parameters for elongations and contractions: (a) **3a** elongation; (b) **4a** elongation; (c) **3b** elongation; (d) **4b** elongation; (e) **3b** contraction; (f) **4b** contraction; (g) **5a** elongation; (h) **6a** elongation; (i) **5b** elongation; (j) **6b** elongation; (k) **5b** contraction; (l) **6b** contraction; (m) **7a** elongation; (n) **8a** elongation; (o) **7b** elongation; (p) **8b** elongation; (q) **7b** contraction; (r) **9a** elongation; (s) **9b** elongation; (t) **10a** elongation; (u) **10b** elongation.

>2.04 Å, the whole molecule undergoes an abrupt conformational change with τ_5 changing value by 95° (Fig. 5c) and τ_4 and τ_6 changing by about 60° with the remaining ring dihedrals showing little change (Table 2, Supplementary data). The resulting ring conformation is near $^{1}S_{3}$. The magnitude of the coefficients reported in Figure 5 quantitatively shows the degree of fit to the respective idealized ring conformations. For example, the 0.876 $^{1}S_{3}$ coefficient for the conformation in Figure 5c is indicative of high degree of this conformation but the 0.341 $^{4}C_{1}$ value shows that it is distorted towards this chair with only a small amount of boat character 0.061 $B_{2,5}$.[23] Subsequent bond elongation leads to a gradual ring conformational change via $^{1,4}B$ and $^{1}S_{5}$ like conformers to a conformation near ^{4}E, see Figure 5d–f. This final conformation is close in conformational space to the final conformation formed from **3a**. This trajectory is also shown in conformational space in Figure 3b. That the conformation after the abrupt conformational change is lower in energy is shown by the energy versus bond length plot in Figure 4b. Once past the minimum, ionization is exothermic

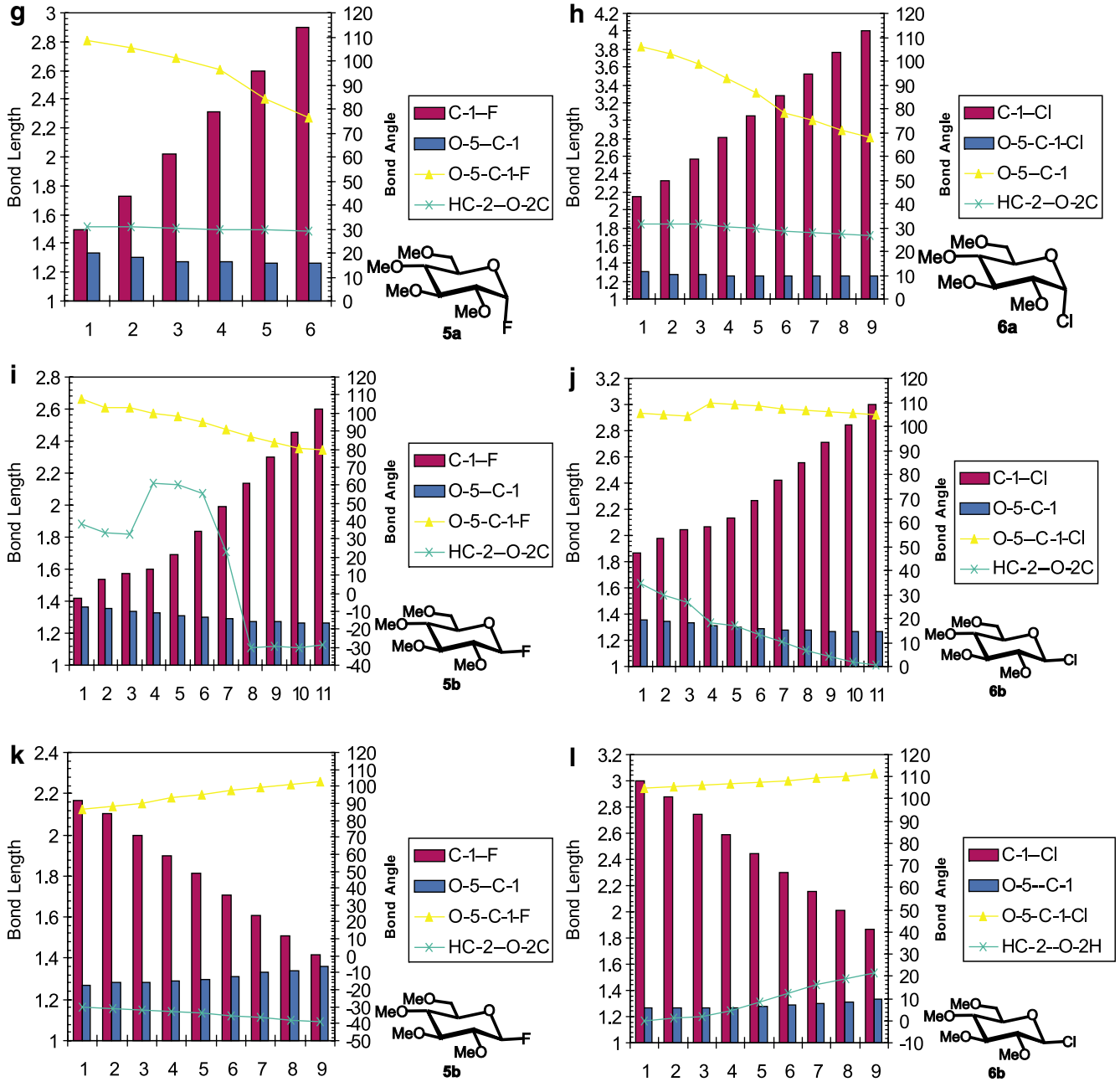

Figure 2 (*continued*)

as in the α-anomer, Figure 4a. It should be noted that this abrupt conformational change precedes appreciable ionization as judged by the geometric parameters in Figure 2c, such as C-1–O-5 bond lengths of 1.30–1.31 Å at the ring conformational change versus 1.26 Å at the species closest to an oxacarbenium ion. The β-triflate **4b** shows an almost identical behaviour with an abrupt conformational change at C-1–O-1 of 1.75 Å and following a very similar series of ring conformations (Fig. 2d). The elongation of this bond had to be terminated earlier than hoped because as this bond lengthened the triflate anion rotated such that a different O–S bond gradually approached C-1. Assuming our DFT calculations adequately model Lemieux's solvolysis conditions, his explanation is partly correct. That is, the β-chloride ionizes differently than the α-chloride but the ultimate species are predicted to be similar. However, it is plausible that under solvolysis conditions the $^{1}S_{3}$ or some conformation intermediate between $^{1}S_{3}$ and ^{4}E, is preferentially attacked from the α-face. This amounts to a model of solvolysis that includes some degree of pre-association of the nucleophile before

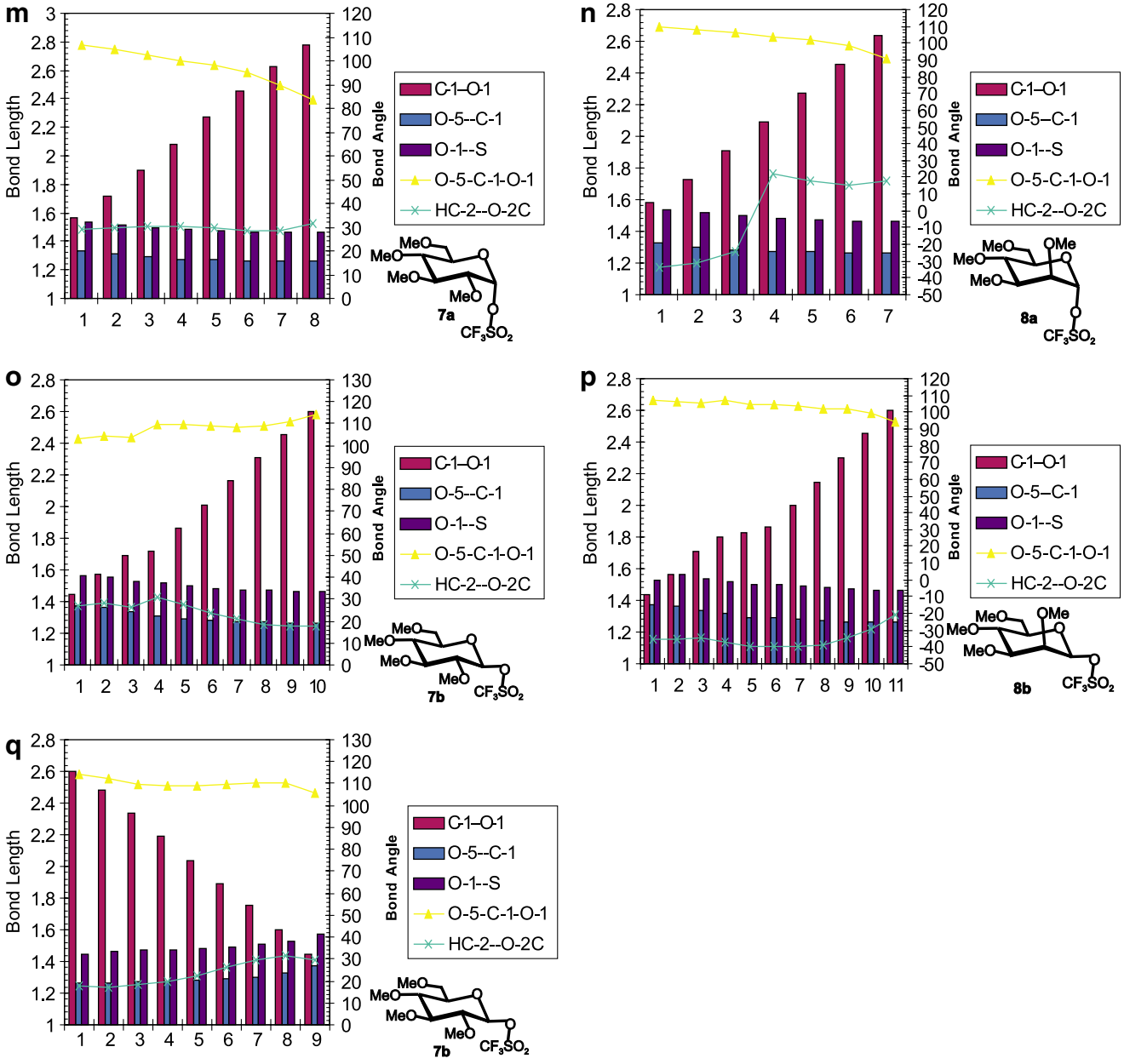

Figure 2 (*continued*)

complete ionization which is not readily detectable from kinetic measurements.[24] Our previous calculations suggested that *gluco* configured ions with $^4H_3$ conformations should be preferentially attacked from the β-face if hydrogen bonding from the nucleophile is possible or from the α-face if it is not.[7b]

Next, we considered the prototypic models of fully protected glycosyl donors, namely 2,3,4,6-tetra-*O*-methyl-α/β-D-glucopyranosyl fluorides (**5ab**), chlorides (**6ab**) and triflates (**7ab**). All three systems exhibited behaviour that is very similar to that of **3ab** and **4ab**. That is, the α-anomers all ionized smoothly to $^4H_3$ conformations (Figs. 2g, 1c and d for **5a** Figs. 2i, k, 1e, f for **5b**) whereas the β-systems showed an abrupt conformational change at C-1–X bond lengths of 1.6 Å (F, **5b**), 2.04 Å (Cl, **6b**) and 1.72 Å (OTf, **7b**). These bond lengths suggest that C-1–X bond lengthening of about 0.2–0.3 Å is sufficient to trigger a conformational change. Snapshots of the bond elongation for triflate **7b** are shown in Figure 6 and as a plot in conformational space in Figure 3c. The consistency of the observation that β-configured sugars at a certain bond length jump to a new conformation and then slowly convert to a conformation near $^4H_3$ with five examples in two systems suggests that this abrupt conformational change is not an artifact. The chloride **6b** is however somewhat anomalous in that it converts to a $^2S_0$ skew boat conformation and does not appreciably change from this conforma-

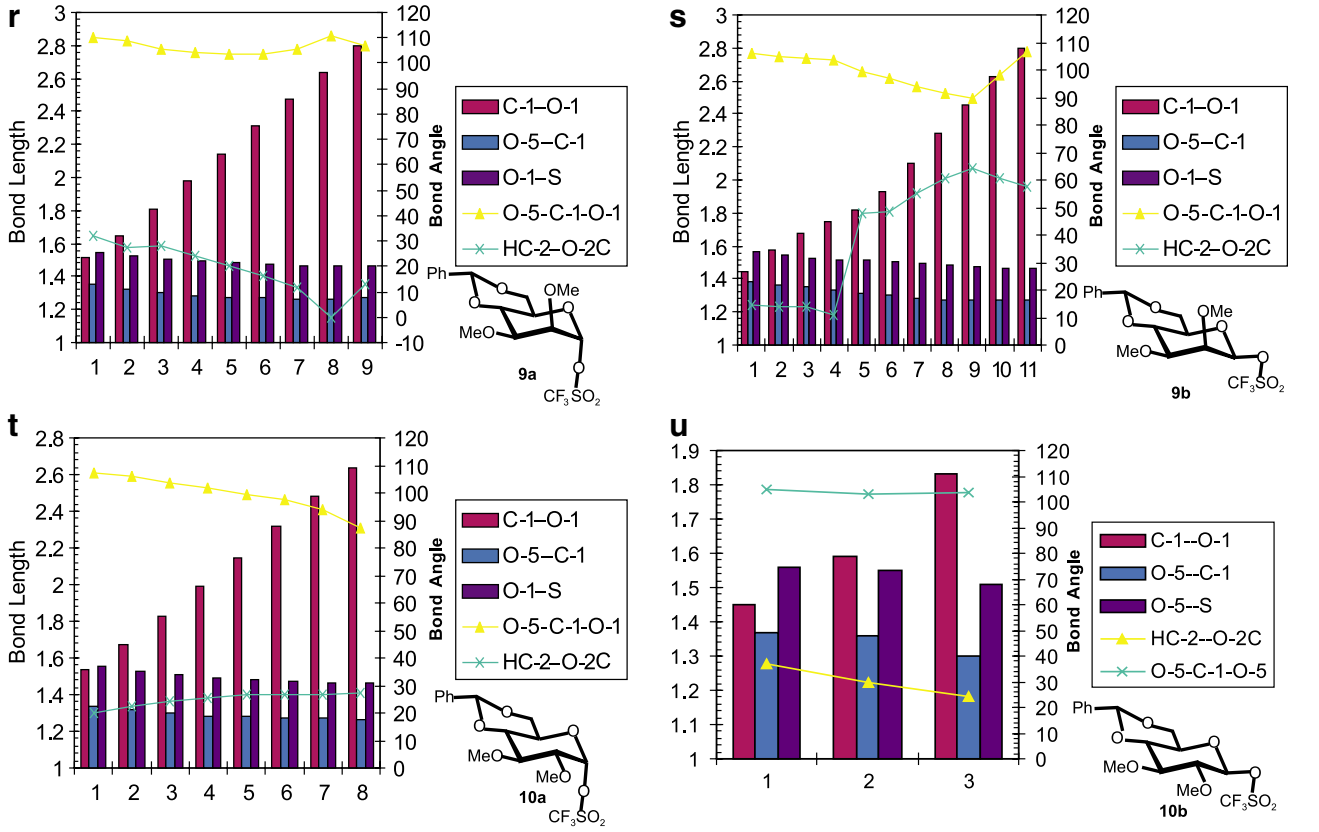

Figure 2 (*continued*)

tion as ionization is increased (Table 3, Supplementary data). Whereas, **5b** converts to near $^{1}S_{3}$ and then to E_{3} and **7b** converts to near E_{3} and then to $^{4}H_{3}$. The bond length versus relative energy plots for **5b** (Fig. 7a and b) are also similar to those for **3ab** with the α-anomers showing a steady exothermicity, whereas the β-anomer drops to a new minimum after the conformational change but otherwise is steadily exothermic too. Thus, the conformational itinerary of the β-anomers depends on the leaving group and the protecting groups. At the intermediate C-1–X bond distances sampled in these calculations there must be some orbital overlap between the leaving group and the sugar which probably subtly affects the pyranosyl ring conformation.[25] The ion–dipole interactions possibly further contribute to these differences.

In all cases, the reverse bond contraction for β-anomers (Fig. 2e for **3b** and Fig. 1f and 2k for **5b**) does not lead to a $^{4}C_{1}$ chair conformation, except for the triflate **7b** (Fig. 2q) as the reversal of the abrupt conformational change does not occur and the essentially neutral sugar species end in a variety of conformations $^{1}S_{5}$ (**3b**), $^{1,4}B$ (**4b**), $^{1}S_{3}$ (**5b**) and $^{2}S_{0}$ (**6b**), Table 3, Supplementary data. Previously, a species near $^{1,4}B$ for penta-*O*-methyl-β-D-glucopyranoside was found to be the secondary minimum which was separated from the minimum $^{4}C_{1}$ chair conformation by a ^{0}E TS with a barrier of about 15 kJ mol^{-1}.[26] Although, the barrier is likely to change depending on the substituent at C-1, a similar pathway would lead to the $^{4}C_{1}$ minimum for all of these species: **3b**, **4b**, **5b** and **6b** (Figs. 8 and 9).

As a further test of the generality of this abrupt ionization, we studied the 2,3,4,6-tetra-*O*-methyl-α/β-D-mannopyranosyl fluoride triflates (**8ab**), see Figure 2n and p. The observed behaviour during C-1–O-1 bond elongation of both anomers was analogous. The α-triflate **8a** smoothly ionizes to an ^{4}E conformation whereas the β-systems showed an abrupt conformational change at C-1–O-1 bond length of 1.83 Å to a $^{1}S_{3}$ conformation and eventually forms a $^{4}H_{3}$ conformation, see Figure 3c.

Finally, we also tried the 4,6-*O*-benzylidene glycopyranosyl systems which for many *manno* configured donors under a variety of glycosylation conditions that likely involve oxacarbenium ion TSs result in preferential formation of β-glycosides.[27] In contrast, many 4,6-*O*-benzylidene glucopyranosyl donors under glycosylation conditions that likely involve oxacarbenium ions lead to neutral α-glycosides.[28] It was previously shown by DFT calculations that the 2,3-di-*O*-methyl-4,6-*O*-benzylidene mannopyranosyl oxacarbenium ion has a stable $B_{2,5}$ conformation while the corresponding *gluco* configured ion an ^{4}E conformation.[29] For the *manno* ion β-facial selectivity was predicted because the ring

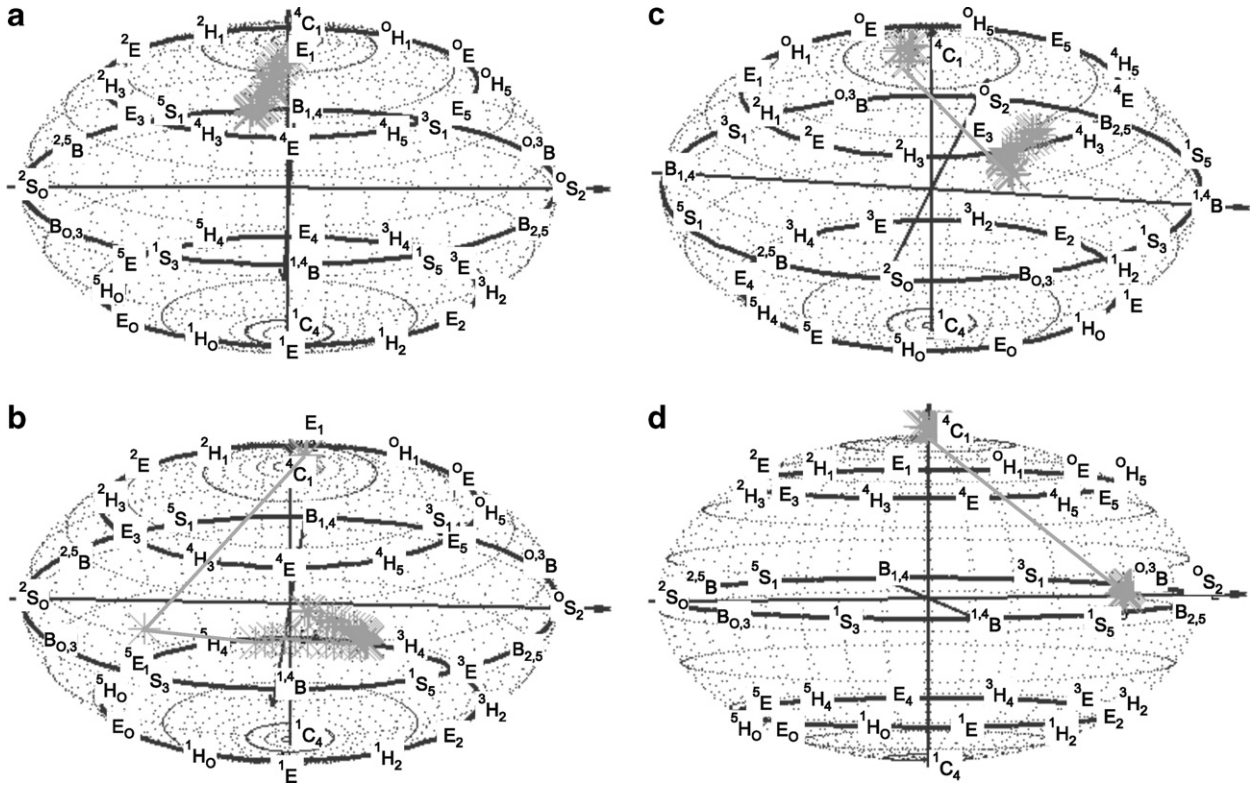

Figure 3. Three-dimensional spherical representation of selected trajectories. The grey lines in (b)–(d) join the points at the large conformational change. The spheres have been individually rotated to best show the trajectory: (a) **3a** elongation; (b) **3b** elongation; (c) **8b** elongation; (d) **9b** elongation.

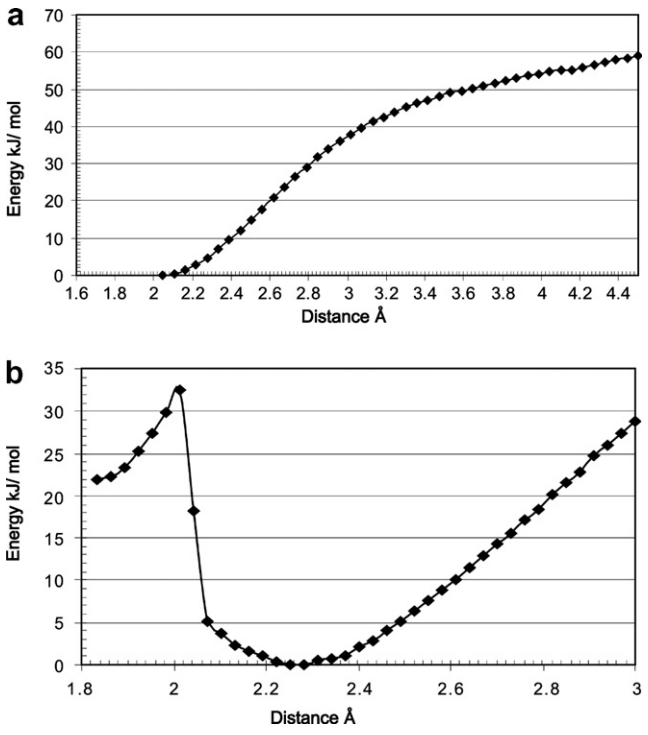

Figure 4. Plots of relative energy versus C-1–Cl bond length for elongations (a) **3a**; (b) **3b**.

could move towards a $^{1}S_{5}$ conformation whereas for the *gluco* ion, α-facial selectivity was predicted because this ring could move towards a $^{4}C_{1}$ chair conformation. These DFT based predictions all depend on the glycosylation reaction proceeding through a fully equilibrated oxacarbenium ion such that the observed glycosides correspond to the most thermodynamically favorable alcohol oxacarbenium ion complex. Such a correlation makes a number of assumptions, including that the reaction barrier between such complexes and neutral products is nearly equivalent. It also assumes negligible effects of nucleophilic pre-association or ion pairing. Both of these effects are expected to play a role in many cases[30] and so the observed correlation between DFT calculations of facially selective complexes and experimentally observed products should be considered as one of the factors to be considered when evaluating key factors controlling glycosylation reactions. Thus, as a partial test of the importance of ion pairing, we calculated the ionization of 2,3-di-*O*-methyl 4,6-*O*-benzylidene-α/β-D-mannopyranosyl triflates (**9ab**) and 2,3-di-*O*-methyl 4,6-*O*-benzylidene-α/β-D-glucopyranosyl triflates (**10ab**), see Figure 2r–u.

For **9ab** the results parallel those above, that is the α-anomer **9a** smoothly ionizes to a $^{4}H_{3}/^{4}E$ conformer and the β-anomer **9b** shows an abrupt conformational

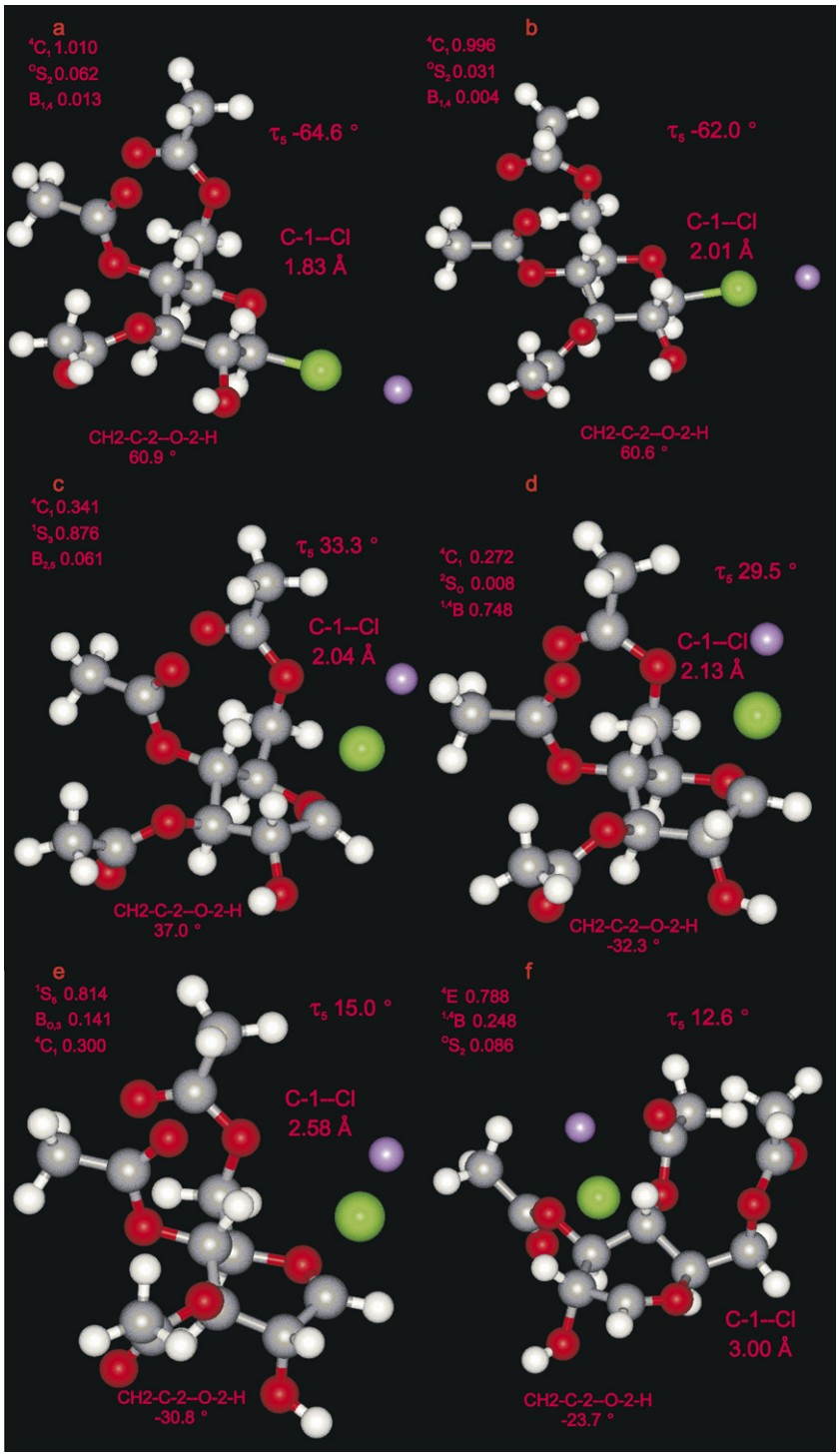

Figure 5. Snapshots of C-1–Cl bond elongation of **3b**. (a) Initial state; (b) short elongation; (c) after conformational change; (d) intermediate conformation after conformational change; (e) near final conformation; (f) final conformation rotated to show the ^4E ring conformation. Element colours: C, grey; H, white; O, red; Cl, green; Li, purple.

change to a $^1S_5$ conformation followed by a slow change to a $B_{2,5}$ conformation, see Figure 3d. However, the two resulting conformations are quite distinct from each other and this result sharply contrasts with those obtained for **3** to **8**. The $B_{2,5}$ conformation closely resembles the one we studied previously, whereas the $^4H_3/^4E$ conformer was not found by us using conventional optimization procedures. It should be noted that these two structures are similar to the ones presented in Ref. 27a For these reasons these two ions without the Tf anion or Li cation were reoptimized and the resulting structures shown to be true minima by frequency calculations,

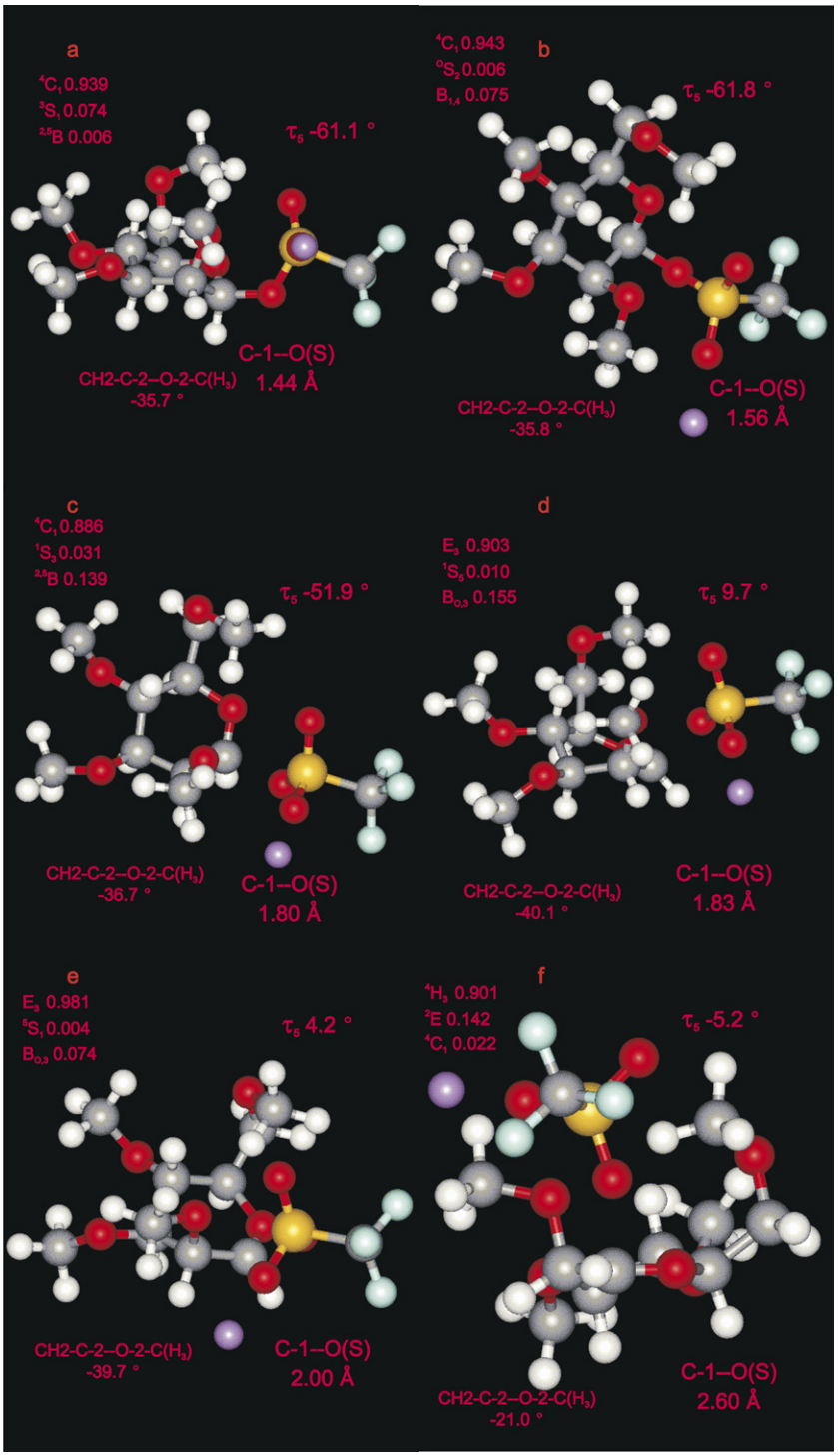

Figure 6. Snapshots of C-1–O-1 bond elongation of **7b**. (a) Initial state; (b) short elongation; (c) just before conformational change; (d) just after conformational change; (e) near final conformation; (f) final conformation rotated to show $^4H_3$ ring conformation. Element colours: C, grey; H, white; O, red; S, yellow; F, pale blue; Li, purple.

see Figure 10. This result shows that even the conformational restriction of the 4,6-benzylidene fused ring is not sufficient to prevent ring inversion and allows the possibility of two conformers of the oxacarbenium ions.

The case for **10ab** is again different with the α-anomer **10a** smoothly ionizing to the previously described ^4E conformation ion. The β-anomer **10b** in spite of numerous attempts with smaller step sizes, different positioning of the Li^+ ion, looser convergence criteria, etc., never converged at a C-1–O-1 bond length where the abrupt conformational change was expected. Whether or not this result represents reality or a failure of the

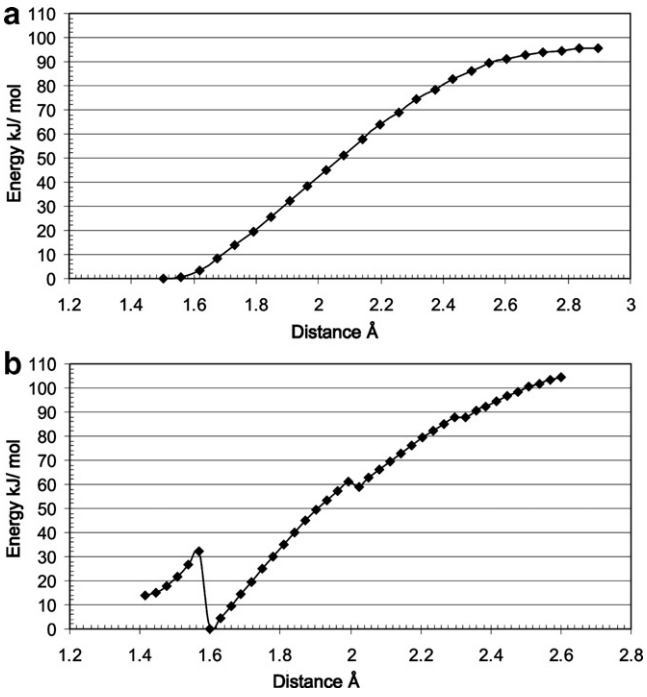

Figure 7. Plots of relative energy versus C-1–F bond length during elongations. (a) **5a**; (b) **5b**.

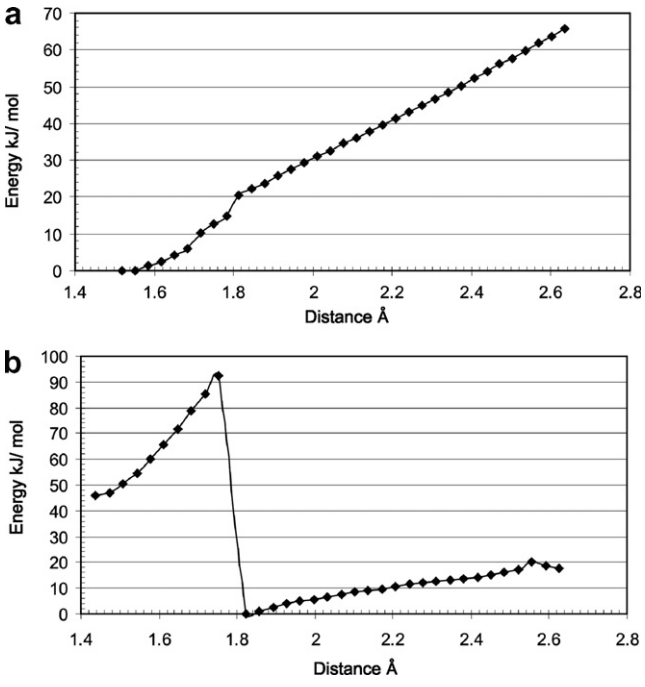

Figure 9. Plot of relative energy versus C-1–O-1 bond length during elongations. (a) **10a**; (b) **10b**.

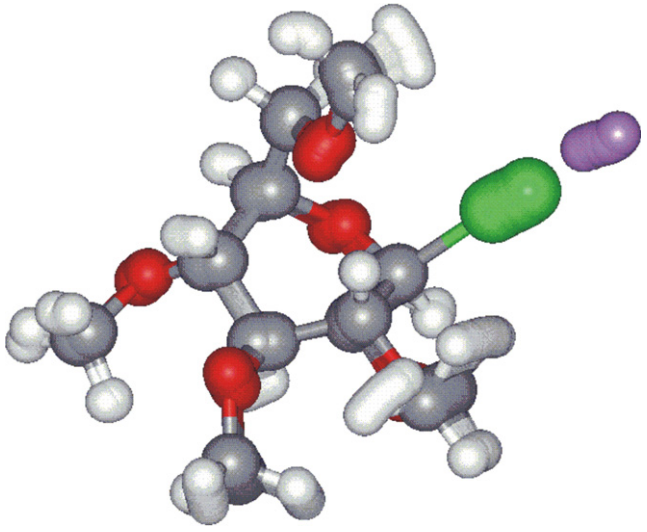

Figure 8. Superposition of snapshots for the C-1–Cl bond contraction of **6b**. Element colours: C, grey; H, white; O, red; Cl, green; Li, purple.

DFT process cannot be deduced from the present data. However, this result does demonstrate that the two anomers ionize differently.

3.2. Specific details—other geometrical parameters

Figure 2a–u contains a selection of geometric parameters that reflect ionization. The C-1–X bond length is used as the driving force for ionization and because at each point it is fixed these calculations are a series of snapshots rather than a dynamic process. The 'real' ionization should be a dynamic process where the C-1–X bond must lengthen but not necessarily in a linear fashion. It is also possible that this lengthening is coupled to other processes, such as ring conformation interconversions and promoter leaving group dynamics, that are not modeled by the present methods. Notably, no indication of ion pairs was found for any system considered here. The closest species to an ion pair detected were the triflates which rotated such that C-1 interacted with two oxygens bonded to sulfur (not shown). Ion pairs have been postulated to be the reactive species in glycosylations especially in the 4,6-benzylidene systems for which **9ab** and **10ab** are prototypes.[30a] The existence of 'free' or 'isolated' oxacarbenium ions, in the sense that neither nucleophile nor counteranions are within bonding distance, has never been conclusively demonstrated outside of a mass spectrometer for the type of systems considered here.[31] The next improvement in our studies should be to include the nucleophile in the anticipation that the partially ionized species studied here should reach a point where they are sufficiently reactive to attract the nucleophile into a productive encounter complex. There is also the possibility that proton transfer from the hydroxylic proton of the alcohol nucleophile to the leaving group is an integral part of some glycosylation reactions as recently suggested by us.[7c] This is an example of the S_Ni mechanism that has been suggested for some retaining glycosyltransferases.[32]

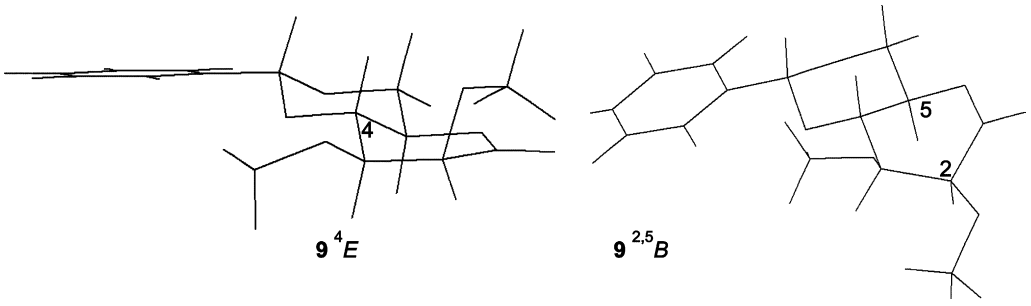

Figure 10. Stick representations of the ^4E and $B_{2,5}$ conformations of ionized **9**.

That the glycopyranosyl ring becomes progressively ionized is evidenced by the shortening of the O-5–C-1 bond to values of 1.26–1.27 Å consistent with a double bond and found previously in QM studies of 'isolated' oxacarbenium ions in the sense described above. The O-5–C-1–X bond angle changes are also suggestive of the formation of oxacarbenium ions. In all cases the initial structures have values near that expected for a sp^3 C of near the tetrahedral values of 109°. For all the α-anomers studied here this value smoothly changes to values near 90° as the C-1–X bond is lengthened. In a few cases, this angle becomes very acute at long C-1–X bond values but this can be traced to interactions of X^- with C–H dipoles. For the β-anomers this gradual decrease is stopped at the abrupt conformational change where a new value is found which, in most cases, gradually changes to near 90° too. Our previous studies of methanol (M) complexes of oxacarbenium ions found the same behaviour where at long C-1–O_M bond distances the O-5–C-1–O_M angle was near 90° and approached 109° at the minima that have appreciable hydronium ion character. Similar species were reported by others during their QM studies of acid-catalyzed hydrolysis of glycosides.[33] This result has obvious implications for modeling the dynamics of glycosylation reactions. Notably, synthetic mimetics of such hydronium ion species like glucosylimidazoles are among the best inhibitors of β-glucosidases known.[2]

The last bond length reported for the triflate species studied here is the O-1–S bond length of the leaving group which shortens as the leaving group becomes more negatively charged. It achieves its minimum length at the same snapshot frames as the O-5–C-1 double bond forms. This results confirms the ionization at the longest C-1–X bond lengths examined here.

Finally the dihedral angle CH-2–C-2–O-2–C (or H for **3ab** and **4ab**) is reported in Figure 2a–u. The previously reported observation that this angle is *syn* (near 0°) in isolated oxacarbenium ions in part prompted the studies presented here because the static calculations did not indicate whether this property is a consequence or the driving force of ionization.[8] This question is of interest to our overall goal of optimizing glycosylation reactions because the judicious choice of protecting groups for O-2 could allow for control of the conformation of the C-2–O-2 torsion and via the mechanism under question, the reactivity of glycosyl donors. This factor also has implications for GPE inhibitor design because it is likely that some of these enzymes take advantage of this stabilizing factor, allowing for both better TS mimics and possible selectivity from similar enzymes that do not use this stabilizing factor. Close examination of Figure 2a–u shows that the C-2–O-2 torsion angle does indeed approach 0° in all cases but only once the glycosyl donors are ionized. The movement about this bond is also evident in many of the figures. The conclusion appears to be that this conformational bias of glycopyranosyl oxacarbenium ions is a consequence of ionization and not a driving force. True mimics of such ions should include this feature in their design and movements towards such ions should also consider this rotation.

4. Conclusion

A prototypic DFT method for studying the ionization of glycopyranosyl donors has been presented. In all cases examined α-anomers ionize smoothly and reversibly to ions with $^4H_3$ or adjacent in conformational space envelope conformations. However, β-anomers exhibit a pre-ionization abrupt conformational change followed by slower changes to ions with similar conformations to their corresponding α-anomers. The exact itinerary depends on both the leaving group and the protecting groups. These observations are consistent with the frequent, but not universal observation that the anomericity of glycosyl donors under glycosylation conditions, where the products do not interconvert, has little or no influence on the stereochemical outcome of the glycosylation reaction.[34] These results suggest two possible scenarios for when this is not to be expected. The first is that partially ionized β-anomers can transiently populate portions of conformational space not readily accessible to α-anomers and if strong nucleophiles can intercept these species such as under solvolysis conditions, then the anomericity of the glycosyl donor may

influence the stereochemical outcome of the reactions plausibly including Lemieux's chlorides **3ab**. The second situation is if the ionization leads to a different conformation of the ion, as found for the torsionally deactivated **9ab**. This second scenario is amenable to control by synthetic chemists as careful control of reaction conditions can channel glycosylation reactions via, for example, α-triflates followed in the case of **9a**, a ^4E ion leading to high stereoselectivity. Obviously, multiple pathways are available under most glycosylation conditions, but careful choice of protecting groups and reaction conditions can lead to highly efficient glycosylations and calculations like these provide a tool for assessing such variables. DFT calculations like the ones presented here are also amenable to detailed studies of GPEs and hence to arriving at not only plausible TS structures but also the motions that lead to the TS. Such information should assist in designing true TS mimics with resulting high inhibition constants.

Acknowledgements

This work was partly supported by the HPC multi scale modeling initiative of the NRC. The author thanks the NRC computer support group (IMSB) for ongoing assistance. This is NRC paper 42519.

Supplementary data

Three tables of data for distinct points of each trajectory are available. Table 1 contains the numbers in Figure 2a–u and for some additional trajectories. Table 2 contains the six ring dihedrals for each point from Table 1 and Table 3 contains the ring descriptors calculated from the torsion angles using the program available at http://www.sao.nrc.ca/ibs/6ring.html. Supplementary data associated with this article can be found, in the online version, at doi:10.1016/j.carres.2007.05.012.

References

1. Schramm, V. I. *Curr. Opin. Struct. Biol.* **2005**, *15*, 604–613.
2. (a) Gloster, T. M.; Meloncelli, P.; Stick, R. V.; Zechel, D.; Vasella, A.; Davies, G. J. *J. Am. Chem. Soc.* **2007**, *129*, 2345–2354; (b) Whitworth, G. E.; Macauley, M. S.; Stubbs, K. A.; Dennis, R. J.; Taylor, E. J.; Davies, G. J.; Greig, I. R.; Vocadlo, D. J. *J. Am. Chem. Soc.* **2007**, *129*, 635–644; (c) Wicki, J.; Williams, S. J.; Withers, S. G. *J. Am. Chem. Soc.* **2007**, *129*, 4530–4531.
3. Vasella, A.; Davies, G. J.; Böhm, M. *Curr. Opin. Chem. Biol.* **2002**, *6*, 619–629.
4. (a) Ducros, V. M.-A.; Zechel, D. L.; Murshudov, G. N.; Gilbert, H. J.; Szabó, L.; Stoll, D.; Withers, S. G.; Davies, G. J. *Angew. Chem., Int. Ed.* **2002**, *41*, 2824–2827; (b) Blériot, Y.; Vadivel, S. K.; Herrera, A. J.; Greig, I. R.; Kirby, A. J.; Sinaÿ, P. *Tetrahedron* **2004**, *60*, 6813–6828; (c) Lorthiois, E.; Meyyappan, M.; Vasella, A. *J. Chem. Soc., Chem. Commun.* **2000**, 1829–1830.
5. Bérces, A.; Nukada, T.; Whitfield, D. M. *Tetrahedron* **2001**, *57*, 477–491.
6. Money, V. A.; Smith, N. L.; Scaffidi, A.; Stick, R. V.; Gilbert, H. J.; Davies, G. J. *Angew. Chem., Int. Ed.* **2006**, *45*, 5136–5140.
7. (a) Ionescu, A. R.; Whitfield, D. M.; Zgierski, M. Z.; Nukada, T. *Carbohydr. Res.* **2006**, *341*, 2912–2920; (b) Nukada, T.; Bérces, A.; Wang, L. J.; Zgierski, M. Z.; Whitfield, D. M. *Carbohydr. Res.* **2005**, *340*, 841–852; (c) Whitfield, D. M.; Nukada, T. *Carbohydr. Res.* **2007**, *342*, 1291–1304.
8. Ionescu, A.; Wang, L.-J.; Zgierski, M. Z.; Nukada, T.; Whitfield, D. M. *ACS Symp. Ser.* **2006**, 302–319.
9. Karaveg, K.; Siriwardena, A.; Tempel, W.; Liu, Z. J.; Glushka, J.; Wang, B. C.; Moremen, K. W. *J. Biol. Chem.* **2005**, *280*, 16197–16207.
10. (a) Nerinckx, W.; Desmet, T.; Claeyssens, M. *Arkivoc* **2006**, *xiii*, 90–116; (b) Lee, J. K.; Bain, A. D.; Berti, P. J. *J. Am. Chem. Soc.* **2004**, *126*, 3769–3776.
11. Mohr, M.; Bryce, R. A.; Hillier, I. H. *J. Phys. Chem. A* **2001**, *103*, 8216–8222.
12. Stubbs, J. M.; Marx, D. *Chem. Eur. J.* **2005**, *11*, 2651–2659.
13. (a) Deslongchamps, P.; Li, S.; Dory, Y. L. *Org. Lett.* **2004**, *6*, 505–508; (b) Andrews, C. A.; Fraser-Reid, B.; Bowen, J. P. *J. Am. Chem. Soc.* **1991**, *113*, 8293–8298.
14. (a) Baerends, E. J.; Ellis, D. E.; Ros, P. *Chem. Phys.* **1973**, *2*, 41–51; (b) te Velde, G.; Baerends, E. J. *J. Comput. Phys.* **1992**, *99*, 84–98; (c) Fonseca Guerra, C.; Snijders, J. G.; te Velde, G.; Baerends, E. J. *Theor. Chim. Acta* **1998**, *99*, 391–403; (d) Versiuis, L.; Ziegler, T. *J. Chem. Phys.* **1988**, *88*, 322–328; (e) Fan, L.; Ziegler, T. *J. Chem. Phys.* **1992**, *96*, 9005–9012.
15. Hricovíni, M. *Carbohydr. Res.* **2006**, *341*, 2575–2580.
16. Vosko, S. H.; Wilk, L.; Nusair, M. *Can. J. Phys.* **1980**, *58*, 1200–1211.
17. Becke, A. D. *Phys. Rev. A* **1988**, *38*, 3098–3100.
18. Perdew, J. P. *Phys. Rev. B* **1986**, *34*, 7506–7516.
19. (a) Lemieux, R. U. *Can. J. Chem.* **1951**, *29*, 1079–1091; (b) Lemieux, R. U. *Adv. Carbohydr. Chem.* **1954**, *9*, 1–57.
20. (a) Smith, D. M.; Woerpel, K. A. *Org. Biomol. Chem.* **2006**, *4*, 1195–1201; (b) Lucero, C. G.; Woerpel, K. A. *J. Org. Chem.* **2006**, *71*, 2641–2647; (c) Shenoy, S. R.; Smith, D. M.; Woerpel, K. A. *J. Am. Chem. Soc.* **2006**, *128*, 8671–8677.
21. Crich, D. *J. Carbohydr. Chem.* **2002**, *21*, 667–690.
22. Callam, C. S.; Gadikota, R. R.; Krein, D. M.; Lowary, T. L. *J. Am. Chem. Soc.* **2003**, *125*, 13112–13119.
23. Whitfield, D. M.; Nukada, T. *ACS Symp. Ser.* **2006**, *932*, 265–300.
24. Bowden, T.; Garegg, P. J.; Maloisel, J. L.; Konradsson, P. *Isr. J. Chem.* **2000**, *40*, 271–277.
25. Berti, P. J.; McCann, J. A. B. *Chem. Rev.* **2006**, *106*, 506–555.
26. Ionescu, A. R.; Bérces, A.; Zgierski, M. Z.; Whitfield, D. M.; Nukada, T. *J. Phys. Chem. A.* **2005**, *109*, 8096–8105.
27. (a) Abdel-Rahman, A. A.-H.; Jonke, S.; El Ashry, E. S. H.; Schmidt, R. R. *Angew. Chem., Int. Ed.* **2002**, *41*, 2972–2974; (b) Weingart, R.; Schmidt, R. R. *Tetrahedron Lett.* **2000**, *41*, 8753–8758; (c) Crich, D.; Sun, S. *Tetrahedron* **1998**, *54*, 8321–8348; (d) Ito, Y.; Ohnishi, Y.; Ogawa, T.; Nakahara, Y. *Synlett* **1998**, 1102–1104.
28. Crich, D.; Cai, W. *J. Org. Chem.* **1999**, *64*, 4926–4930.

29. Nukada, T.; Bérces, A.; Whitfield, D. M. *Carbohydr. Res.* **2002**, *337*, 765–774.
30. (a) Crich, D.; Vinogradova, O. *J. Org. Chem.* **2006**, *71*, 8473–8480; (b) Crich, D.; Chandrasekera, N. S. *Angew. Chem., Int. Ed.* **2004**, *43*, 5386–5389.
31. (a) Kovacik, V.; Hirsch, J.; Thölmann, D.; Grützmacher, H.-F. *Org. Mass. Spectrom.* **1991**, *26*, 1085–1088; (b) Suzuki, S.; Matsumoto, K.; Kawamura, K.; Suga, S.; Yoshida, J.-I. *Org. Lett.* **2004**, *6*, 3755–3758; (c) Boebel, T. A.; Gin, D. Y. *J. Org. Chem.* **2005**, *70*, 5818–5826.
32. Ly, H. D.; Lougheed, B.; Wakarchuk, W. W.; Withers, S. G. *Biochemistry* **2002**, *41*, 5075–5085.
33. Blériot, Y.; Genre-Grandpierre, A.; Imberty, A.; Tellier, C. *J. Carbohydr. Chem.* **1996**, *15*, 985–1000.
34. (a) Whitfield, D. M.; Douglas, S. P. *Glycoconjugate J.* **1996**, *13*, 5–17; (b) Paulsen, H. *Angew, Chem., Int. Ed. Engl.* **1982**, *21*, 155–175; (c) Demchenko, A. V. *Curr. Org. Chem.* **2003**, *7*, 35–79; (d) Kochetkov, N. E. In *Studies in Natural Products Chemistry*; Rahman, A., Ed.; Elsevier, 1994; Vol. 14, pp 201–266.